

## Double Scattering Experiment with 96-Mev Protons\*

KARL STRAUCH

Harvard University, Cambridge, Massachusetts

(Received March 2, 1955)

By using 96-Mev protons, a double scattering experiment has been performed with a variety of targets and scattering angles. The observed values of the asymmetry  $e$  in the intensity of the second-scattered beam are small. For instance with carbon as a first and second scatterer, and scattering angles of  $20^\circ$  the observed value of  $e = +3.6 \pm 1.6$  percent. It is concluded that the polarization  $P$  decreases rapidly with decreasing energy below 130 Mev.

### I. INTRODUCTION

DOUBLE scattering experiments performed with a variety of targets and using protons with energies of about 130 Mev and higher have shown pronounced azimuthal asymmetries  $e$  in the intensity of the second scattered beam. This indicates that a high degree of polarization can be achieved by scattering of protons from nuclei. It has also been shown that the magnitude of the asymmetry  $e$  and therefore of the degree of polarization increases as the scattering events become more nearly "elastic."<sup>1</sup>

The purpose of the investigation described here was twofold: to measure the magnitude of the asymmetry  $e$  in an energy region not previously investigated, and to gain more precise information on the nature of the "elastic" events responsible for the large polarization effects. Unfortunately the second part of this program could not be carried out since the magnitude of  $e$  turns out to be too small in the accessible energy region.

In previous double scattering experiments, the first scattering had been carried out inside the cyclotron tank. In this investigation, both scatterings were carried out with the external beam for the following reasons:

(1) Since nothing was known about the magnitude of the polarization below 130 Mev at the time this experiment was started, the greatest possible flexibility seemed desirable. The method used allowed the rapid variation of both the first and second scattering angles.

(2) When high-energy protons interact with a nucleus small momentum transfers are possible which leave the target nucleus in low-lying excited states.<sup>2</sup> One way to assure that the majority of both scattering events are truly elastic is to use a primary beam whose energy width is less than the separation between the ground and first excited state of the target nucleus. In the case of carbon, this separation is 4.4 Mev so that at the Harvard cyclotron only the external beam (energy 96 Mev, width 2 Mev) fulfills the requirement.

(3) No serious interference occurred with other experiments in progress at the same time.

\* Supported by the joint program of the Office of Naval Research and the U. S. Atomic Energy Commission.

<sup>1</sup> de Carvalho, Marshall, and Marshall, Phys. Rev. **96**, 1081 (1954); J. M. Dickson and D. C. Salter, Nature **173**, 946 (1954).

<sup>2</sup> K. Strauch and W. F. Titus, Phys. Rev. **95**, 854 (1954).

The main disadvantages of the use of the external beam to carry out both scatterings arise from the small intensity of this beam. As a result, the angular resolution is relatively poor and at certain scattering angles an "inhomogeneity correction" must be applied.

### II. EXPERIMENTAL ARRANGEMENT

The internal cyclotron beam is multiple coulomb scattered by an uranium target into a magnetic channel which extracts a fraction of the beam from the cyclotron (Fig. 1). After analysis and focusing by a slit system and an auxiliary magnet, a 96-Mev proton beam is available outside the shielding with an intensity of  $5 \times 10^5$  protons per second per cm<sup>2</sup>. It has been verified experimentally that this beam is unpolarized.

After emerging from a vacuum pipe through a defining slit, the external beam traversed an ionization chamber monitor and a brass antiscattering slit  $S1$  before encountering the first target  $T1$  (see Fig. 2). The first scattered beam passed through scintillation counters  $A$  and  $B$  (placed at one third the distance  $D$  from  $T1$ ) before reaching the second target  $T2$  placed at a distance  $D$  from  $T1$ . The line passing through the geometric centers of the targets at  $T1$  and  $T2$  will be called "apparatus axis;" it makes an angle  $\theta_1$  with the direction of the external proton beam. Protons scattered by  $T2$  were detected by two identical telescopes 1 and 2 placed symmetrically on either side of the apparatus axis at angles of  $+\theta_2$  and  $-\theta_2$ . The brass shields  $S2$  minimized the number of protons that reached the

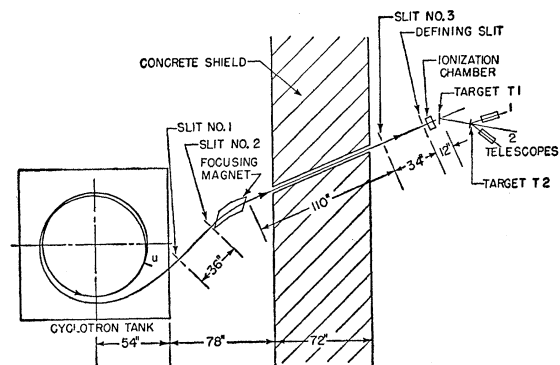


FIG. 1. Arrangement for bringing the external beam to the experimental area.

telescopes either by single scattering in  $T1$  and air, or by a double scattering not involving  $T2$ .

The scattering and counting equipment was mounted on a platform that could be rotated around a vertical axis passing through the center of  $T1$ . The angles  $\theta_1$  and  $\theta_2$  could be varied with a reproducibility of better than 0.03 degrees. Target  $T1$  was always placed at an angle of  $90^\circ - \frac{1}{2}\theta_1$  with respect to the external beam direction.

The telescopes 1 and 2 consisted each of 5 scintillation counters  $C_1$  through  $G_1$  and  $C_2$  through  $G_2$ , spaced so that absorbers could be inserted in front of  $C$  and between  $F$  and  $G$ . The first-scattered beam was defined by the size of the external beam at  $T1$  ( $\frac{3}{4}$ -in. width and 1-in. height) and the size of  $T2$  (1 in.  $\times$  4 in.); the second-scattered beams were defined by the dimensions of  $T2$  and scintillators  $F_1$  and  $F_2$  (2 in.  $\times$  4 in.) respectively. The distance between  $T2$  and  $F_1$  (or  $F_2$ ) will be called  $d$ . The whole scattering and counter assembly was rigidly constructed so that even though  $D$ ,  $d$ ,  $\theta_1$ , and  $\theta_2$  could be varied, and  $T1$  and  $T2$  could be rapidly removed, the apparatus was kept symmetrical around its axis to the necessary tolerances. This fact was checked experimentally by using the steep angular dependence of elastically scattered protons.

Each counter consisted of a  $\frac{1}{8}$ -in. thick plastic scintillator and a 1P21 photomultiplier whose output was fed directly into a diode bridge type double coincidence circuit.<sup>3</sup> Fast coincidence pairs  $AD_1$ ,  $BE_1$ ,  $C_1F_1$ ,  $C_1G_1$ ,  $AD_2$ ,  $BE_2$ ,  $C_2F_2$ ,  $C_2G_2$  were available and these were mixed in slow coincidence circuits whose output corresponded to  $ABC_1D_1E_1F_1$ ,  $ABC_1D_1E_1F_1G_1$ ,  $ABC_2D_2E_2F_2$ , and  $ABC_2D_2E_2F_2G_2$  coincidences, hereafter called  $A-F_1$ ,  $A-G_1$ ,  $A-F_2$ , and  $A-G_2$  coincidences respectively.

All telescope readings were normalized to a standard amount of charge collected in the ionization chamber placed in the external beam.

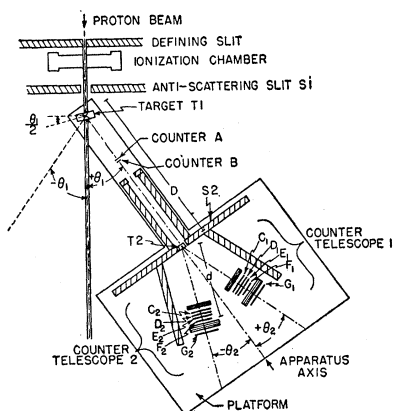


Fig. 2. The double scattering apparatus.

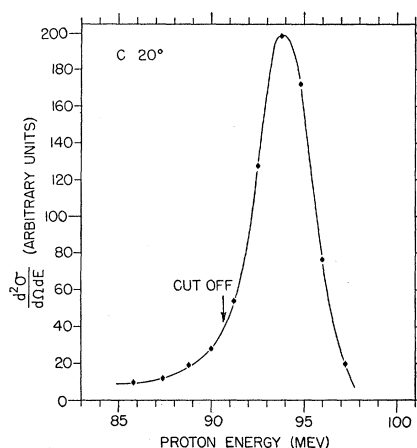


Fig. 3. Energy distribution of protons scattered at  $20^\circ$  from a carbon target. The intrinsic energy width of 2 Mev of the incident beam is broadened by the energy resolution of the telescope.

### III. EXPERIMENTAL PROCEDURE

The use of two telescopes allowed the simultaneous measurement of two independent values of the asymmetry. Consider first telescope 1 only. The asymmetry  $e(\theta_1, \theta_2)$  for a given set of first and second scattering angles  $\theta_1$  and  $\theta_2$  can be measured by keeping  $\theta_1$  constant and determining the number of double scattered protons at the angles  $+\theta_2$  and  $-\theta_2$ . Alternately it is possible to keep  $\theta_2$  constant and to take measurements at first scattering angles of  $+\theta_1$  and  $-\theta_1$  (see Fig. 2). This second method turned out to be the most convenient. Readings with telescope 1 determined  $e(\theta_1, \theta_2)$  as follows:

$$e(\theta_1, \theta_2) = \frac{R_1(+\theta_1, +\theta_2) - R_1(-\theta_1, +\theta_2)}{R_1(+\theta_1, +\theta_2) + R_1(-\theta_1, +\theta_2)}, \quad (1)$$

where for instance  $R_1(+\theta_1, +\theta_2)$  represents the normalized double scattering counting rate of telescope 1 when the first and second scattering angles are  $+\theta_1$  and  $+\theta_2$  respectively (the position of telescope 1 in Fig. 2).

Another set of readings was taken simultaneously with telescope 2 from which an independent value  $e(-\theta_1, -\theta_2)$  could be obtained:

$$e(-\theta_1, -\theta_2) = \frac{R_2(-\theta_1, -\theta_2) - R_2(+\theta_1, -\theta_2)}{R_2(-\theta_1, -\theta_2) + R_2(+\theta_1, -\theta_2)}. \quad (2)$$

From symmetry considerations it follows that:

$$e(\theta_1, \theta_2) = e(-\theta_1, -\theta_2) \quad (3)$$

and the final value of  $e$  was obtained by taking the average of the two independent determinations.

Due to this averaging procedure, small geometric misalignments could not affect the measured value of  $e$ , at least to first-order terms. Actually it is believed that all but one of the alignments (this one to be

<sup>3</sup> K. Strauch, Rev. Sci. Instr. 24, 283 (1953).

discussed below) could be made accurately enough so as to have no appreciable effect on  $e(+\theta_1, +\theta_2)$  or  $e(-\theta_1, -\theta_2)$  individually.

Each run was carried out in five steps.

(1) The apparatus was aligned by photographically centering the external beam on the apparatus axis with  $\theta_1$  set to  $0^\circ$ . This alignment could be done accurately; however, the geometric center and the intensity center of gravity of the external beam do not necessarily overlap. Any possible difference between these two centers can be time dependent, since the beam intensity distribution over the first target depends on the energy distribution of the internal cyclotron beam which is known to vary slightly with time. The readings at  $\pm\theta_1$  were therefore alternated in short cycles and as a result of this and the use of the averaging procedure just outlined the final value of  $e$  is not believed to have been affected by small geometric beam fluctuations.

(2) After plateaux for all critical electronic settings had been obtained, the telescope efficiencies were rapidly compared to an accuracy of 1 percent by alternately moving each telescope into the first scattering beam by setting  $\theta_2=0$ .

(3) The energy of the external beam was measured with one of the telescopes set at the  $\theta_2=0$  position by measuring the difference between  $A-G$  and  $A-F$  coincidence rates as a function of thickness of absorbers placed in front of counter  $C$ . A typical result is shown in Fig. 3. Enough absorbers were then inserted into each telescope so that  $A-G_1$  and  $A-G_2$  coincidences represent protons whose energy is less than about 3 Mev below the elastic peak value when both scatterings take place at the center of the targets. The required absorbers were divided into two sets placed as shown in Fig. 2 so that the  $A-F_1$  and  $A-F_2$  coincidence rates could have included some double scattering events in which a

considerable amount of momentum was transferred during a collision.

(4) With the apparatus in position to detect double scattering events (as shown in Fig. 2), accidental and spurious coincidences due to the high counting rates in counters  $A$  and  $B$  were measured by inserting behind  $B$  an absorber large enough to just cover the scintillator and thick enough to stop all protons. With all targets used and at all angles investigated, such coincidences were found to be negligible. These tests also indicated that no appreciable number of double scattering events of the type  $p-n-p$  were detected.

(5) For a given set of targets  $T1$  and  $T2$ , the normalized counting rates  $R_1(+\theta_1, +\theta_2)$ ,  $R_1(-\theta_1, +\theta_2)$  and  $R_2(+\theta_1, -\theta_2)$ ,  $R_2(-\theta_1, -\theta_2)$  were then obtained by subtracting the background as follows:

$$R(\theta_1, \theta_2) = R'(\theta_1, \theta_2) - R''(\theta_1, \theta_2) - R'''(\theta_1, \theta_2), \quad (4)$$

where  $R'(\theta_1, \theta_2)$  = normalized counting rate with targets  $T1$  and  $T2$  in place,  $R''(\theta_1, \theta_2)$  = normalized counting rate with target  $T1$  in place, target  $T2$  removed, and  $R'''(\theta_1, \theta_2)$  = normalized counting rate with target  $T1$  removed, target  $T2$  in place. This method of background subtraction slightly overemphasized the importance of the background since with the target in place some of the background protons should have lost enough energy in these targets to fall below the telescope threshold. However the background was small enough so that the final value of the asymmetry  $e$  was but little affected: values of  $e$  obtained by the method of subtraction outlined above differed on the average by only 50 percent of the statistical uncertainty from values of  $e$  obtained without any background subtraction. A set of typical data is shown in Table I. Some of the background counts were taken for shorter periods of time than the counts obtained with both scatterers in place. However in Table I all counts have been normalized to the same monitor reading.

#### IV. THE INHOMOGENEITY CORRECTION

In general, the differential cross section for elastic (and "nearly" elastic) scattering decreases rapidly with increasing scattering angle. As a result, the intensity of the first scattered beam is not homogenous over the surface of the second target  $T2$ : The center of gravity of protons striking  $T2$  does not lie on the apparatus axis, but is deviated toward the external beam direction. As can be seen by considering the experimental geometry (Fig. 2), this "inhomogeneity effect" produces a negative contribution to the observed asymmetry  $e$ , whether or not polarization is present. This contribution can be minimized by using as large a distance  $D$  between the first and second target as permitted by intensity considerations.

However, there are some angular regions over which the differential elastic scattering cross section for 96-Mev protons is essentially flat. For a light element such as carbon, such a region, centered around  $8.5^\circ$ ,

TABLE I. Data obtained in 4 cycles with  $T1:Be$ ,  $T2:Be$ ,  $\theta_1=\theta_2=20^\circ$ ,  $D=30$  in.,  $d=11$  in.

	$A-F$ coincidences	$A-G$ coincidences
$R_1'(20^\circ, 20^\circ)$	$1844 \pm 43$	$1011 \pm 32$
$R_1''(20^\circ, 20^\circ)$	$386 \pm 28$	$78 \pm 13$
$R_1'''(20^\circ, 20^\circ)$	$30 \pm 9$	$18 \pm 8$
$R_1(20^\circ, 20^\circ)$	$1428 \pm 52$	$915 \pm 35$
$R_1'(-20^\circ, 20^\circ)$	$1783 \pm 42$	$1047 \pm 32$
$R_1''(-20^\circ, 20^\circ)$	$320 \pm 25$	$48 \pm 10$
$R_1'''(-20^\circ, 20^\circ)$	$15 \pm 7$	$6 \pm 5$
$R_1(-20^\circ, 20^\circ)$	$1448 \pm 50$	$993 \pm 34$
$R_2'(20^\circ, -20^\circ)$	$1516 \pm 39$	$954 \pm 31$
$R_2''(20^\circ, -20^\circ)$	$120 \pm 15$	$26 \pm 7$
$R_2'''(20^\circ, -20^\circ)$	$18 \pm 8$	$6 \pm 5$
$R_2(20^\circ, -20^\circ)$	$1387 \pm 42$	$922 \pm 32$
$R_2'(-20^\circ, -20^\circ)$	$1670 \pm 41$	$998 \pm 32$
$R_2''(-20^\circ, -20^\circ)$	$184 \pm 19$	$52 \pm 10$
$R_2'''(-20^\circ, -20^\circ)$	$6 \pm 5$	$3 \pm 4$
$R_2(-20^\circ, -20^\circ)$	$1480 \pm 45$	$943 \pm 33$

TABLE II. Summary of experimental results.

T1	T2	$\theta_1$	$\theta_2$	D (in- ches)	d (in- ches)	$E_1$ (Mev)	$E_1$ (Mev)	$E_2$ (Mev)	$E_2$ (Mev)	Eth (Mev)	A-F		A-G		
											$e_{\text{obs}}$ %	$e$ %	Eth (Mev)	$e_{\text{obs}}$ %	$e$ %
C	C	8.5°	18°	60	11	86.4	14.9	68.2	9.7	10.4	-1.2±1.9	-1.2±1.9	2.5	+1.7±2.0	+1.7±2.0
C	C	15°	15°	60	14	86.6	15.5	68.1	9.6	19.6	-0.4±2.1	+0.2±2.1	2.6	+0.2±1.9	+0.7±1.9
C	C	15°	15°	30	14	86.6	15.5	68.1	9.6	19.6	+0.5±1.8	+1.8±1.8	2.6	+1.6±1.6	+3.0±1.6
C	C	20°	20°	30	11	86.6	16.0	67.6	10.0	18.9	-3.0±1.7	+2.5±1.7	3.9	-1.9±1.6	+3.6±1.6
Be	Be	20°	20°	30	11	87.3	14.2	69.7	9.3	21.0	+1.3±1.6	+4.5±1.6	3.3	-1.5±1.8	+3.1±1.8
C	Cu	8.5°	18°	60	11	86.4	14.9	63.4	20.7	11.0	+0.3±1.6	+0.3±1.6	2.2	+0.3±1.8	+0.3±1.8
Cu	Cu	26°	18°	30	11	85.7	16.3	61.7	21.2	9.9	+4.9±1.6	+4.9±1.6	3.6	+4.3±1.7	+4.3±1.7

is produced by interference between Coulomb and nuclear potential scattering. In heavier elements, a flat region exists at the top of the second diffraction maxima which in the case of copper occurs at 26°. When these special values are used for the first scattering angle  $\theta_1$ , no inhomogeneity effect exists and the asymmetry due to proton polarization can be measured directly.

At other angles an "inhomogeneity correction" must be applied to the observed asymmetries. This was done by using the angular distribution of the first and second scattered beam to calculate the expected contribution to  $e$  of the inhomogeneity effect, and then subtracting this contribution from the observed asymmetry  $e$ . The angular distributions were measured in each case with the same targets and the same beam energy as occurred in the double scattering experiment. The magnitude of the correction can be seen from Table II. Although this is difficult to estimate, it is believed that the additional uncertainty introduced in some of the final values of  $e$  by the inhomogeneity correction is at most as large as the statistical errors shown in Table II.

## V. RESULTS AND DISCUSSION

Table II summarized the asymmetries obtained in this investigation. The column headings have the following meaning:  $T1$  and  $T2$ : first and second scattering targets,  $\theta_1$  and  $\theta_2$ : first and second scattering angles,  $D$ : distance between  $T1$  and  $T2$ ,  $d$ : distance between  $T2$  and defining counter,  $E_1$  and  $\Delta E_1$ : average energy and spread in this energy at which the first scattering occurred due to target 1 thickness,  $E_2$  and  $\Delta E_2$ : average energy and spread in this energy at which the second scattering occurred due to target 2 thickness,  $E_{\text{th}}$ : the lowest energy proton that was detected had an energy  $E_{\text{th}}$  below the elastic peak energy,  $e_{\text{obs}}$ : observed value of the asymmetry, and  $e$ : value of the asymmetry after inhomogeneity correction had been applied where necessary.

The most striking conclusion to be drawn from the results presented in Table II is that the asymmetry  $e$  due to polarization of protons of less than 96 Mev is very small for the targets and at the angles investigated. This conclusion holds for both  $A-G$  and  $A-F$  coincidence events, that is events in which the majority of both scattering events were elastic and events that

also included some inelastic scatterings. The errors shown are of statistical origin only. It is difficult to get accurate estimates of other sources of error but they might conceivably add up to the magnitude of the observed asymmetries.

It does not appear probable that the small size of the observed asymmetries are only due to an unfortunate choice of angles and targets. Large asymmetries have been observed with higher energy protons using the same targets and scattering at corresponding angles. The small size of the asymmetries seems to be due to the decreased energy at which the two scatterings took place in this investigation.

The asymmetry  $e$  directly determines an average value of  $P$ , the polarization that would be produced by scattering an unpolarized beam on the substance in question. The average is taken over the energy region covered by the first and second scattering. For instance, with two carbon scatterers and both scattering angles at 20°, the asymmetry  $e = P_1 P_2 = P_{\text{av}}^2 = 3.6 \pm 1.6$  percent and this determines  $P_{\text{av}} = 19 \pm 13$  percent for carbon at 20°.

This value should be compared to  $P \approx 75$  percent obtained at 130 Mev at Harwell with carbon at 16°.<sup>4</sup> The magnitude of this decrease in the value of  $P$  is typical of the variation for the other target elements.

Since the observable quantity  $e$  varies as  $P_1 P_2$ , it is much easier to measure accurately small values of  $P_2$  by using a first scattering in which  $P_1$  is large. This has since been done at Harwell<sup>4</sup> and at Chicago<sup>5</sup> by performing the first scattering above 100 Mev, reducing the energy of the first-scattered beam (highly polarized) by passing it through absorbers and then doing the second scattering at a lower energy. By using the Harwell results, it is possible to estimate the asymmetries that should have been observed in this experiment and the agreement is satisfactory.

It should be pointed out that Fermi's theory<sup>6</sup> for the polarization of elastically scattered protons correctly predicts the magnitude of the observed asymmetries. For  $\theta_1 = \theta_2 = 20^\circ$ ,  $E_1 = 86$  Mev and  $E_2 = 68$  Mev, this

<sup>4</sup> Dickson, Rose, and Salter (private communication, 1954).

<sup>5</sup> Heiberg, Kruse, Marshall, Marshall, and Solnitz, Phys. Rev. **97**, 250 (1955).

<sup>6</sup> E. Fermi, Nuovo cimento **11**, 407 (1954).

theory predicts an asymmetry of 3.8 percent or 6.5 percent depending on whether potential values determined from total neutron cross sections by Shapiro and Teem<sup>7</sup> or by Taylor<sup>8</sup> are used.

<sup>7</sup> I. I. Shapiro and J. M. Teem (private communication).

<sup>8</sup> T. B. Taylor, Phys. Rev. **92**, 831 (1953).

The author is indebted to Dr. L. Marshall and Dr. B. Rose for communicating their results before publication. Mr. J. Calame, Mr. F. Federighi, Mr. G. Gerstein, and Mr. J. Niederer helped during the long periods of data taking and greatly contributed to the success of this investigation.

## Alternative Interpretations of Slow-Neutron Cross Sections\*

O. KOFOED-HANSEN†

Columbia University, New York, New York

(Received October 26, 1954; revised manuscript received March 3, 1955)

The many-level formula of the theory of neutron resonance cross sections developed by Feshbach, Peaslee, and Weisskopf has been applied to the lowest resonances in Ag and Au. It is concluded that the approximations involved in the derivation of the usual Breit-Wigner one-level formula may lead to larger deviations in the determination of the constants in this formula than indicated by the usually applied statistical errors. In particular, in the present work a fit is obtained with a nuclear radius given as  $1.47A^{1/3} \times 10^{-13}$  cm.

### INTRODUCTION

A CONSIDERABLE amount of information has been amassed in the studies of neutron capture and scattering cross sections at very low energies. The experimental data are usually interpreted in terms of the resonance formula.<sup>1</sup>

$$\sigma_t = \sigma_p + \sigma_s + \sigma_c$$

$$= \sum_i 4\pi R^2 g_i \left\{ 1 + \frac{1 - 2 \operatorname{Re} f_0}{(\operatorname{Re} f_0)^2 + (kR - \operatorname{Im} f_0)^2} + \frac{-\operatorname{Im} f_0/kR}{(\operatorname{Re} f_0)^2 + (kR - \operatorname{Im} f_0)^2} \right\} \quad (1,a)$$

$$\cong \sigma_p + \frac{\sigma_{s0}\Gamma^2 + A(E - E_0)}{4(E - E_0)^2 + \Gamma^2} + \frac{\sigma_{c0}\Gamma^2(E_0/E)^{1/2}}{4(E - E_0)^2 + \Gamma^2}, \quad (1,b)$$

where  $\sigma_p$  (potential),  $\sigma_s$  (scattering), and  $\sigma_c$  (capture) are  $\sum_i 4\pi R^2 g_i$  times the corresponding terms in the curly bracket. The formula (1,a) is the phenomenological description of low-energy neutron cross sections. The expression is valid only when  $kR \ll 1$ , where  $k$  is the neutron wave number and where it has been assumed that the nucleus has a relatively well-defined radius  $R$ . Because  $kR \ll 1$ , only  $S$ -neutrons contribute to  $\sigma_t$ . The factors  $g_i$  are the statistical weights corresponding to the two possible spin states of the

compound nucleus occurring whenever the target nucleus has a spin  $\neq 0$ . The function  $f_0$  is the logarithmic derivative of the radial wave function for the neutron evaluated at the nuclear radius  $R$ .  $f_0$  has been split into its real part  $\operatorname{Re} f_0$  and its imaginary part  $\operatorname{Im} f_0$ . ( $n, \gamma$ ) reactions are responsible for the existence of the imaginary part of  $f_0$ .

In deriving the usual one-level Breit-Wigner formula (1,b) from (1,a), FPW develop  $\operatorname{Re} f_0$  in a Taylor series in the neutron energy  $E$  and around the resonance energy  $E_0$  where  $\operatorname{Re} f_0 = 0$ . In this expansion, only the first significant term is kept:

$$\operatorname{Re} f_0 = (d \operatorname{Re} f_0 / dE)_{E_0} (E - E_0) + \dots \quad (2)$$

In this way, the constants in (1,b) are defined by

$$\begin{aligned} \sigma_p &= 4\pi R^2, \\ \Gamma^2 &= [(kR - \operatorname{Im} f_0)^2]_{E_0} / [(\frac{1}{2} d \operatorname{Re} f_0 / dE)^2]_{E_0}, \\ \sigma_{s0}\Gamma^2 &= g_i 4\pi R^2 \{ (1/kR)_{E_0} (-\operatorname{Im} f_0)_{E_0} / [(\frac{1}{2} d \operatorname{Re} f_0 / dE)^2]_{E_0} \}, \\ \sigma_{c0}\Gamma^2 &= g_i 4\pi R^2 / [(\frac{1}{2} d \operatorname{Re} f_0 / dE)^2]_{E_0}, \\ A &= -g_i 16\pi R^2 / (\frac{1}{2} d \operatorname{Re} f_0 / dE)_{E_0}. \end{aligned} \quad (3)$$

The validity of (2) is limited to a distance which is small compared to the level spacing. Nevertheless, the observed resonance cross sections often show an excellent agreement with the shape of (1,b) even at distances far off resonance. The experimental results are often represented in terms of the constants in (3). Here for example  $\sigma_p$ , the energy-independent part of the cross section, has been used in order to determine the nuclear radius<sup>2</sup> and it has been concluded that  $\operatorname{Ag}^{107}$

\* This work was supported by the U. S. Atomic Energy Commission.

† On leave from the Institute for Theoretical Physics, University of Copenhagen, Copenhagen, Denmark.

<sup>1</sup> We use the formulation given by Feshbach, Peaslee, and Weisskopf, Phys. Rev. **71**, 143 (1947) (referred to as FPW). See also J. M. Blatt and V. F. Weisskopf, *Theoretical Nuclear Physics* (John Wiley and Sons, Inc., New York, 1952).

<sup>2</sup> J. Tittman and C. Sheer, Phys. Rev. **83**, 746 (1951); C. Sheer and J. Moore, Phys. Rev. **98**, 565 (1955).